ELSEVIER

Surface Science 511 (2002) 112–120

SURFACE SCIENCE

www.elsevier.com/locate/susc

Structure change of Ni(1 ML)/Si(1 1 1) by post-annealing observed by atomic force microscopy, ion scattering and photoelectron spectroscopy

Y. Hoshino [a], T. Nishimura [a], Y. Taki [a], Y. Asami [a], K. Sumitomo [b], Y. Kido [a,*]

[a] *Department of Physics, Ritsumeikan University, Kusatsu-shi Noji-higashi, Shiga-ken 525-8577, Japan*
[b] *NTT Basic Research Laboratory, Atsugi, Kanagawa-ken 243-0198, Japan*

Received 31 October 2001; accepted for publication 8 March 2002

Abstract

Structure change of Ni(1 ML: 7.83×10^{14} atoms/cm^2)/Si(1 1 1) by post-annealing was observed by reflection high energy electron diffraction, atomic force microscopy (AFM), medium energy ion scattering (MEIS) and photoelectron spectroscopy. The AFM observation showed dramatic change of the surface morphology after the Ni deposition at room temperature (RT) followed by annealing at 400, 600, 700 and 800 °C for 2 min in an ultrahigh vacuum. MEIS using 70 keV He$^+$ ions analyzed the depth profiles of Ni and the crystallographic structure of the Ni-composites formed by annealing. The valence band and the Si-2p and Ni-3p core level analyses using synchrotron-radiation light showed that the NiSi phase appeared by 1 ML-Ni deposition at RT and both NiSi and NiSi$_2$ islands were formed by annealing at 400 °C. Annealing at 600 and 700 °C led to growth of the B-type NiSi$_2$ islands with height of four and six Si–Ni–Si triple layers. After annealing at 800 °C, three-fourth of the deposited Ni atoms were dissipated from the surface and the dominant surface structure was the 1×1-ring clusters accompanied by a small amount of $\sqrt{19} \times \sqrt{19}$ phase. The present analysis clearly showed the structure change of Ni (1 ML)/Si(1 1 1) by post-annealing and provided the information about the kinetics for the Ni–Si system. © 2002 Published by Elsevier Science B.V.

Keywords: Medium energy ion scattering (MEIS); Photoelectron spectroscopy; Atomic force microscopy; Silicides; Semiconducting films; Surface structure, morphology, roughness, and topography

---

1. Introduction

Epitaxial metal silicides have many applications in the areas of Si-based semiconductor devices [1–5]. In general, forming epitaxial silicide thin films with good quality can be very difficult and variety of deposition techniques have been developed. A key parameter to form defect free epitaxial films is the lattice match of the silicide to the single crystal Si substrate. As well known, NiSi$_2$/Si has the smallest lattice mismatch of 0.4%. Of course, prior to the application, there are many requirements to be cleared such as low resistivity, thermal stability and good adhesion etc. Among many metal silicides, NiSi$_2$, CoSi$_2$ and TiSi$_2$ are the most promising candidates as the MOS-FET gate electrodes.

---

[*] Corresponding author. Tel.: +81-77-561-2710; fax: +81-77-561-2657.
E-mail address: ykido@se.ritsumei.ac.jp (Y. Kido).

0039-6028/02/$ - see front matter © 2002 Published by Elsevier Science B.V.
PII: S0039-6028(02)01557-1

In order to obtain good quality of silicide films with an abrupt interface, it is essential to control the initial stage of the silicidation process at the interface. For example, metal silicides with CaF_2 structure tend to form A- and B-type epitaxial layers on Si(1 1 1) [6,7]. The former is a continuation of the Si lattice planes and the latter results from a single stacking fault caused by a 180° rotation of the silicide with respect to the Si substrate. Significant difference of the Schottky barrier height between the A- and B-type $NiSi_2$ was reported by Tung [8]. The orientation of epitaxial $NiSi_2$ layers depends upon annealing procedure, deposition rate and temperature, initial amount of Ni deposited and wafer preparation [7,9]. Preferential growth of B-type $NiSi_2$ by solid phase epitaxy (SPE) of submonolayer Ni deposited at room temperature (RT) is due to kinetic and energetic advantages but the detailed mechanism is still unknown.

There are some reports on the atomic structure and morphology of the Si(1 1 1) surface onto which Co or Ni with submonolayer or less was deposited [10–20]. Van Loenen et al. [11] reported that the Ni_2Si islands grew for Ni-deposition more than 2.5 ML at RT and Si-rich silicides were formed for fewer Ni coverage. According to Porter et al. [12], the B-type $NiSi_2$ was grown by 0.12 ML Ni deposition at RT. It was also reported that RT-deposition followed by annealing produced $NiSi_2$, NiSi-like islands, $\sqrt{3} \times \sqrt{3}$, $\sqrt{19} \times \sqrt{19}$ structures and 1 × 1-ring cluster (RC) [17–21]. According to Parkin et al. [18], Ni deposition of 0.08 ML (1 ML: 7.83×10^{14} atoms/cm^2) at RT followed by annealing at 860 °C and quenching produced 1 × 1-RC phase and for Ni coverage of 0.2 ML the $\sqrt{19} \times \sqrt{19}$ structure appeared. For higher Ni coverage they found the formation of $NiSi_2$ islands from Auger and reflection high energy electron diffraction (RHEED) measurements. Using scanning photoelectron spectromicroscopy (SPESM), Gregoratti et al. [20,21] performed two-dimensional mapping of the reaction products on the submonolayer-Ni deposited Si(1 1 1) surface. The characteristic phase formation after post-annealing is due to the high solubility of Ni into the Si substrate at temperatures higher than about 750 °C and to the surface segregation of the dissolved Ni atoms during the cooling process [17,20]. Despite the several reports mentioned above, the systematic picture is still insufficient concerning the morphology, diffusion kinetics, the phase and crystallographic structure of the reaction products and so on.

In this study, it is intended to obtain clearer pictures of the atomic and electronic structures of ultra-thin Ni deposited Si(1 1 1) surface before and after post-annealing. Structure change by post-annealing associated with the growth kinetics of silicidation and surface reconstruction is particularly concerned. For this purpose, we employed RHEED, photoelectron spectroscopy (PES) with synchrotron radiation (SR) light, medium energy ion scattering (MEIS) and an atomic force microscope (AFM). The PES analysis identifies the chemical bonds of reaction products and MEIS gives absolute amount of Ni near surface regions together with the crystallographic structure of the Ni-composites. The Ni deposition was made at RT with a Knudsen cell (K-cell) and an infra-red radiation (IR) heating system was used for annealing. Except for AFM observation, all the measurements were performed in situ under an ultra-high vacuum (UHV) condition ($\leqslant 2 \times 10^{-10}$ Torr).

2. Experiment

The experiment was carried out at the beamline named SORIS, which was connected to the storage ring of a 575 MeV electron synchrotron working at Ritsumeikan University. The structure and performance of the SORIS beamline were described elsewhere [22,23]. We employed n-type Si(1 1 1) substrates with an off-set angle less than 0.1° and prepared clean 7 × 7 surfaces by usual chemical treatment followed by heating at 1200 °C for 15 s by IR. Temperature was measured with a thermocouple covered with thin silica-based glass to avoid the silicidation. The uncertainty of measured temperatures is estimated to be ±30 °C at most. The RHEED observation together with Auger electron spectroscopy confirmed the clean 7 × 7 surfaces without any contaminations. Then 1 ML Ni was deposited onto the clean Si(1 1 1)-7 × 7 surface at RT with the K-cell at a rate of 0.13 ML/min. Post-annealing was performed at 400, 600, 700 and 800 °C for 2 min by IR heating in the base pressure of 4×10^{-10} Torr. The B-type $NiSi_2$ layer with thickness 45 Å grown on Si(1 1 1) was prepared for comparison. The temperature-raising and cooling rates were 100 °C/min and 100–120 °C/min, respectively. This condition is similar to that for the usual solid phase epitaxy of transition metal silicides. The amount of Ni was measured by MEIS with a toroidal electrostatic analyzer (ESA). Rutherford backscattering (RBS) using 2.0 MeV He^+ beams calibrated the absolute amount of Ni. The as-deposited and annealed samples were transferred from the preparation chamber equipped with the K-cells and the IR and RHEED systems to the MEIS and PES chambers without exposure to the air.

We performed the ultra-violet photoelectron spectroscopy (UPS) and the Si-2p and Ni-3p core level analyses with SR-photon energy of 40, 114 and 130 eV. The emitted photoelectrons were detected with a hemispherical ESA with a mean radius of 137.9 mm. MEIS with 70 keV He^+ ions analyzed not only the depth profile of Ni but also the crystallographic structure of the reaction products on the surface using the ion-channeling and blocking effects. The surface morphology of the as-deposited and post-annealed samples was observed ex situ in the air by AFM.

3. Results and discussion

Table 1 shows the RHEED patterns observed for the as-deposited and post-annealed samples. The sharp 7×7 spots became weak and fuzzy by 1 ML-Ni deposition at RT. After annealing at 400 °C, the 1×1, $\sqrt{3} \times \sqrt{3}$ and $\sqrt{19} \times \sqrt{19}$ phases appeared. The appearance of the latter two phases is consistent with the result observed by a scanning tunneling microscope (STM) [19]. The weak 1×1 spots are probably due to the formation of a small amount of $NiSi_2$. Post-annealing at 600 and 700 °C led to a clear 1×1 pattern originating from $NiSi_2$ islands, whose formation would be confirmed later by MEIS and UPS. The 1×1 pattern accompanied by weak $\sqrt{19} \times \sqrt{19}$ spots appeared by post-annealing at 800 °C.

Fig. 1 shows the AFM images observed for the clean 7×7 surface, as-deposited, 400-, 600-, 700- and 800 °C-annealed Ni(1 ML)/Si(1 1 1). For the clean surface, regular steps together with step bunching are clearly seen. The deposited Ni atoms coalesced to make ridge-like stripes perpendicular to steps and also formed fine clusters in some places. The average height of the ridges is 1.5 Å. Three fine particles seen are SiC (confirmed by RHEED), which tend to be created when the vacuum is worse ($\geqslant 5 \times 10^{-9}$ Torr) during the surface cleaning process at high temperatures. By 400 °C-annealing, Ni atoms coalesced to form islands on upper terrace sides at step edges. The height of relatively large islands is 6.5 Å, corresponding to two Si–Ni–Si-triple layers of $NiSi_2$. In fact, Vrijmoeth et al. [15] showed that the $NiSi_2$ (1 1 1) surface was terminated by a Si–Ni–Si triple layer. At this stage, both NiSi (smaller) and $NiSi_2$ (larger) islands were formed. From the shape and location, the larger islands are expected to be a

Table 1
Results obtained by RHEED, AFM, PES and MEIS for Ni(1 ML)/Si(1 1 1), as deposited and annealed at 400, 600, 700 and 800 °C for 2 min

Sample	RHEED patterns	AFM	PES	MEIS
As-deposited	7×7 (weak)	Ridge-like stripes with height of 1.5 Å accompanied by small islands	NiSi	Amorphous Ni: 1.0 ML
400 °C	$1 \times 1 + \sqrt{19} \times \sqrt{19} + \sqrt{3} \times \sqrt{3}$ (weak)	Small islands plus large ones with height of 2-triple layers	$NiSi + NiSi_2$	Partially epitaxial Ni: 0.81 ML
600 °C	1×1	Triangular-shaped islands with height of 4-triple layers	$NiSi_2$	Epitaxial B-type $NiSi_2$ Ni: 0.53 ML
700 °C	1×1	Triangular- and polygon-shaped islands with height of 6-triple layers	$NiSi_2$	Epitaxial B-type $NiSi_2$
800 °C	$1 \times 1 + \sqrt{19} \times \sqrt{19}$ (weak)	Very fine clusters	$NiSi_2$ (small amount)	Polycrystal-like Ni: 0.27 ML

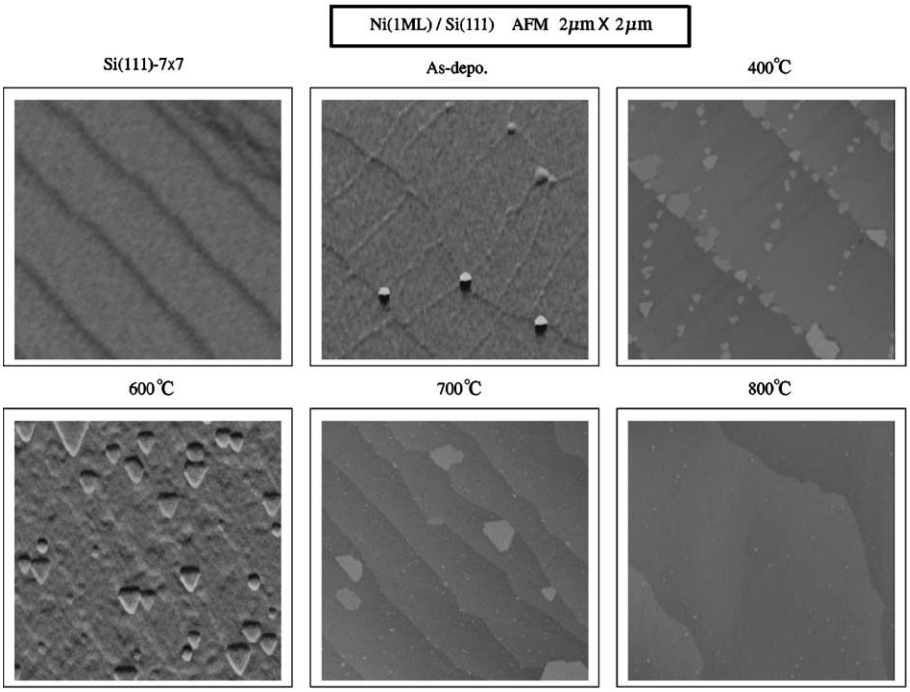

Fig. 1. AFM images (2 μm × 2 μm) observed for clean 7 × 7 surface, as-deposited, 400-, 600-, 700- and 800 °C-annealed samples.

precursor state of the $NiSi_2$ islands observed for the 600 °C-annealed sample. Both phase formation will be confirmed by UPS analysis later. Thus it is reasonable to consider the smaller islands located still on the terraces to be the NiSi phase. Annealing at 600 °C led to epitaxial growth of atomically flat $NiSi_2$ islands with a triangular shape. These islands are just the B-type $NiSi_2(1\,1\,1)$, which is determined by MEIS, as will be shown later. The bases of the triangles are located along step edges and the height is almost constant (12.5 Å) corresponding to 4-triple layers. After annealing at 700 °C, large islands of $NiSi_2$ were still alive and small ones seem being dissolved and diffused into the substrate. The diffused Ni atoms partly segregated to the surface during slow cooling to RT and probably formed the RC structure [17] and fine $NiSi_2$ clusters. Annealing at 800 °C dissolved the $NiSi_2$ island completely and surface segregation occurred during the cooling process [17,20]. The segregated Ni atoms created a small amount of the $\sqrt{19} \times \sqrt{19}$ structure and fine Ni-composite clusters (probably $NiSi_2$). The dominant 1×1 RHEED pattern suggests the formation of the 1×1-RC phase. It must be noted that the amount of Ni at the surface is 0.27 ML (see Table 1) and the Ni coverages of the $\sqrt{19} \times \sqrt{19}$ and 1×1-RC structures are 0.16 and 0.14 ML [17,18], respectively, if the surface is terminated completely with each corresponding structure. Therefore, the residual Ni atoms of about 0.1 ML probably exist as fine $NiSi_2$ clusters. Recently, Gregoratti et al. [20] showed that two types of islands of NiSi and $NiSi_2$ in coexistence with the 1×1-RC phase were formed for Ni deposition of 1 ML at RT then annealed at 877 °C for 15 s and subsequently at 677 °C for 45 s followed by slow cooling to RT (100 °C/min).

In order to identify the phase of reaction products, we performed the PES analysis with 40, 114 and 130 eV photon beams. Fig. 2 shows the valence band (VB) spectra measured for the clean $Si(1\,1\,1)$-7×7 surface, as-deposited, 400-, 600- and 800 °C-annealed samples. For comparison, the VB spectrum for the B-type $NiSi_2$ (45 Å) grown on $Si(1\,1\,1)$ was also measured. Three dashed lines indicate the binding energies of the Ni_2Si(-1.3 eV),

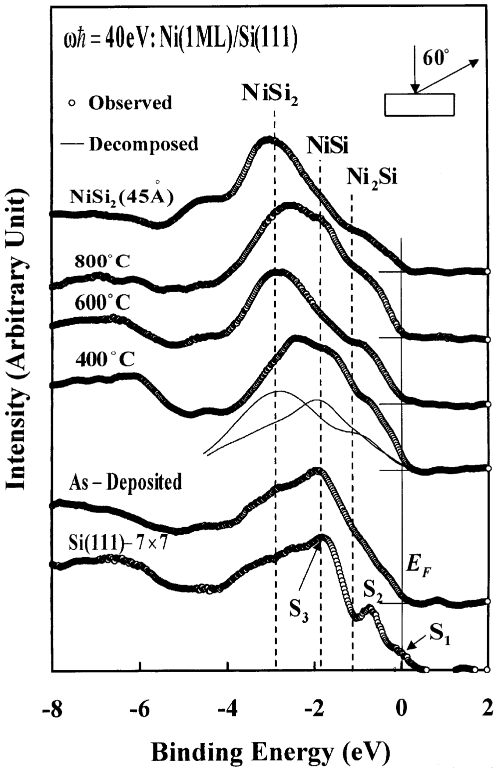

Fig. 2. UPS spectra measured with 40 eV SR-photons for clean 7 × 7 surface, as-deposited, 400-, 600-, 700- and 800 °C-annealed samples. The B-type $NiSi_2$ layers with thickness of 45 Å was prepared by 15 ML-Ni deposition on Si(1 1 1)-7 × 7 surface at RT followed by post-annealing at 650 °C for 5 min. Growth of the B-type $NiSi_2$(1 1 1) was confirmed by MEIS using the blocking effect. S_1 (adatom dangling bonds), S_2 (rest-atom dangling bonds) and S_3 (adatom back bonds) denote the surface state levels for the Si(1 1 1)-7 × 7 [27]. SR-photons were incident along surface normal direction and photoelectrons emitted to 60° were detected. Binding energy values are scaled from Fermi level. The VB spectrum observed for the 400 °C-annealed sample is decomposed into two components (thin solid curves) from the as-deposited (NiSi) and 600 °C-annealed ($NiSi_2$) samples.

NiSi(−1.85 eV) and $NiSi_2$ (−3.15 eV) [24–26]. By deposition of 1 ML-Ni at RT the 7 × 7 surface states (S_1, S_2 and S_3) disappeared and the NiSi phase appeared. The surface states, S_1, S_2 and S_3 were assigned to the adatom dangling bonds, rest-atom dangling bonds and adatom back bonds, respectively [27]. These surface peaks immediately disappear by O_2-exposure of 10 L(1 L: 10^6 Torr s) [28]. In fact, the 7 × 7-RHEED pattern became very weak after the Ni-deposition. Thus the peak around −2 eV in the VB spectrum for the as-deposited sample comes primarily from the NiSi phase. Coexistence of the NiSi and $NiSi_2$ phases are seen after post-annealing at 400 °C and annealing at 600 °C led to formation of the $NiSi_2$ phase only. The broad peak in the VB spectrum for the 400 °C-annealed sample is decomposed into two components corresponding to those observed for the as-deposited and 600 °C-annealed samples. The spectrum for the 600 °C-annealed sample is quite similar to that for $NiSi_2$ (45 Å)/Si(1 1 1). The VB spectrum obtained for the 800 °C-annealed sample indicates that the primary structure is no longer the $NiSi_2$ phase, although a small amount of the $NiSi_2$ phase may still exist.

We also measured the Si-2p and Ni-3p core levels at photon energy of 130 and 114 eV, respectively. Background was subtracted by the Shirley method [29]. Fig. 3 depicts the Si-2p spectra

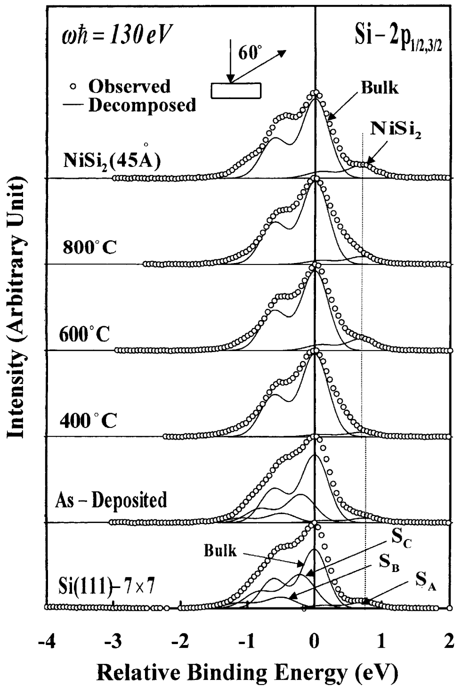

Fig. 3. Si-2p core level spectra observed for 130 eV photons incident along the surface normal and emission angle of 60°. S_A, S_B and S_C denote the surface components of Si(1 1 1)-7 × 7 and are assigned to the rest-atoms, the adatoms and the atoms bonding to the adatoms, respectively [27]. The Si-$2p_{3/2}$ peak for Si(1 1 1)-7 × 7 is taken as the origin of the binding energy.

measured at normal incidence and detection angle of 60° with respect to the surface normal. The Si-2p spectrum from the clean 7 × 7 surface is decomposed into bulk and surface components (S_A, S_B, S_C). The peak (S_A) with a 0.8 eV lower binding energy than the bulk peak was assigned to the rest-atom [27]. The other surface components S_B and S_C correspond to the adatoms and the atoms binding to the adatoms, respectively [27]. Theses surface components are still seen for the as-deposited sample, although the intensities are significantly weakened. In fact, as mentioned earlier, the weak 7 × 7 RHEED pattern was observed. Formation of the $NiSi_2$ phase created a new peak with a 0.7 eV lower binding energy than the bulk peak ($NiSi_2$ (45 Å)/Si(1 1 1)). This $NiSi_2$ signal is clearly seen for the 600 °C-annealed sample as well. A small amount of $NiSi_2$ is also seen for the 400- and 800 °C-annealed samples. The Ni-3p spectra were observed at the same incidence and detection geometry (Fig. 4). The Ni-$3p_{3/2}$ peak seen for 600 °C-annealed sample was slightly shifted by 0.4 eV toward the higher binding energy side compared with that observed for the as-deposited and 400 °C-annealed samples. This binding energy shift is responsible for phase change from NiSi to $NiSi_2$. In fact, Gregoratti et al. [21] also observed a similar binding energy shift between NiSi and $NiSi_2$ islands by SPESM. By post-annealing at 800 °C, the Ni-3p peak was broadened and strongly weakened in spite of the residual Ni amount of 0.27 ML estimated from MEIS, as will be shown below.

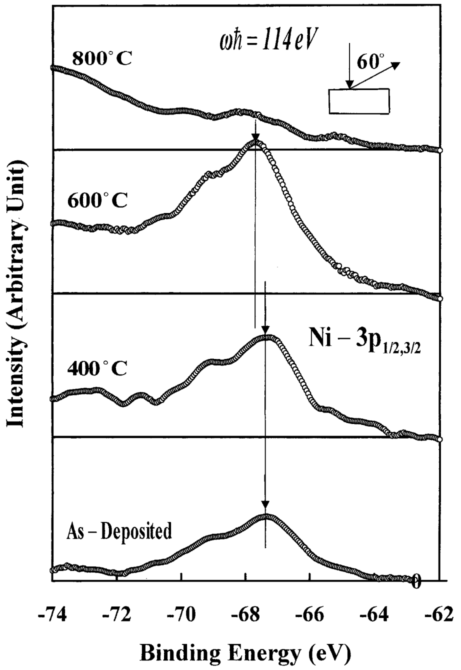

Fig. 4. Ni-3p core level spectra observed with photon energy of 114 eV for as-deposited, 400-, 600- and 800 °C-annealed samples. Binding energy values are scaled from Fermi level.

The MEIS measurement was carried out using 70 keV He^+ ions under two scattering geometries with the same scattering angle (54.74°), (i) aligned $[0 0 \bar{1}]$-incidence and $[1 1 \bar{1}]$-emergence and (ii) random incidence and emergence. Fig. 5(a) and (b) shows the aligned and random MEIS spectra for as-deposited, 400-, 600- and 800 °C-annealed

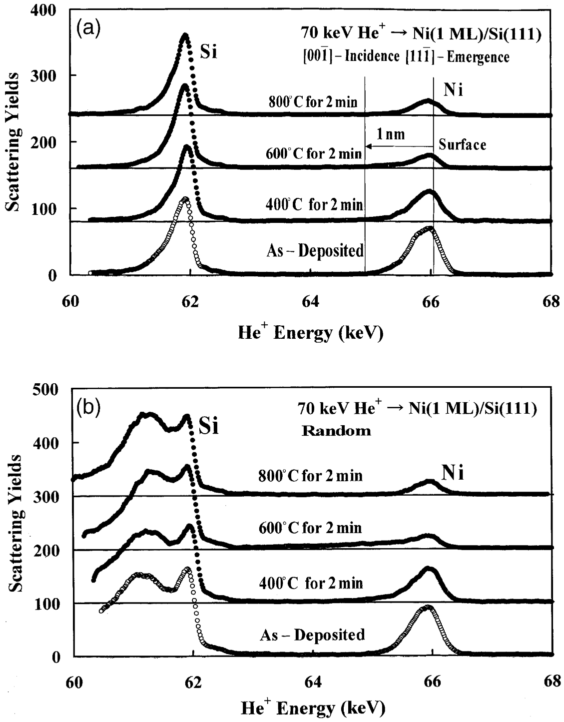

Fig. 5. (a) Double alignment MEIS spectra for 70 keV He^+ incident along $[0 0 \bar{1}]$-axis and backscattered to $[1 1 \bar{1}]$-axis and (b) random MEIS spectra. Scattering angle and plane are 54.74° and $(1 \bar{1} 0)$, respectively. In case (b), scattering plane was rotated by 5.5° off from $(1 \bar{1} 0)$.

samples. Here, the energy scale of 1 keV corresponds to the depth scale of 9 Å for Si. The total amounts of Ni located from the top surface down to 25 Å in depth are determined from the random spectra to be 1.0 ± 0.02, 0.81 ± 0.04, 0.53 ± 0.02, 0.27 ± 0.024 ML for as-deposited, 400-, 600- and 800 °C-annealed samples, respectively. The long tail of the Ni spectrum seen for the 600 °C-annealed sample is responsible for the formation of $NiSi_2$ islands with height of 4-triple layers (12.5 Å), which was observed by AFM. Apparently the tail is reduced in the aligned spectrum compared with that in the random one owing to the ion shadowing effect for the epitaxial $NiSi_2$ layers. In the case of 400 °C-annealing, a small tail is also seen in the random spectrum and is reduced in the aligned spectrum. It indicates the existence of thin $NiSi_2$ islands (2-triple layers), which was expected from the AFM observation. In order to determine which type of epitaxial layer was formed, A-type or B-type, we performed polar scans around the $[1\,1\,\bar{1}]$- and $[\bar{1}\,\bar{1}\,5]$-axis in the $(1\,\bar{1}\,0)$ plane of the Si(1 1 1) substrate for 600- and 700 °C-annealed samples (see Fig. 6). Here, the incident angle was fixed to 62° with respect to surface normal (random incidence) and the detection angle was varied around the above axes. Fig. 7(a) shows the scattering yields from the second layer Ni atoms (including a small contribution from the fifth layer Ni) and from the Si substrate as a function of polar angle around the $[1\,1\,\bar{1}]$-axis with respect to the surface normal ([1 1 1]-axis). It must be noted that our toroidal ESA has an excellent energy resolution of $\Delta E/E = 9 \times 10^{-4}$, which allows a layer-by-layer analysis near surface regions [30,31]. If the A-type $NiSi_2$ islands are grown, the $[1\,1\,\bar{1}]$-blocking dip would be seen for the scattering components from the second layer Ni for the polar-scan spectrum around the $[1\,1\,\bar{1}]$-axis of the Si substrate. On the other hand, growth of the B-type $NiSi_2$ would yield the $[1\,1\,\bar{1}]$-blocking dip in the $[\bar{1}\,\bar{1}\,5]$ direction of the Si substrate. In the case of the polar scan around the $[1\,1\,\bar{1}]$-axis, we have no blocking dip, as shown in Fig. 7(a). On the other hand, the polar scan around the $[\bar{1}\,\bar{1}\,5]$-axis of the Si substrate gives the clear $[1\,1\,\bar{1}]$-blocking dip (Fig. 7(b)). In this polar scan, a small $[\bar{1}\,\bar{1}\,5]$-blocking dip is seen for the scattering components from the Si substrate. Here, we note that the plus sign of the polar angle is taken as rotation toward the $[1\,1\,\bar{2}]$-axis of the Si substrate and the $[1\,1\,\bar{1}]$- and $[\bar{1}\,\bar{1}\,5]$-axes make a same angle of 70.53° with respect to the [1 1 1]-axis (surface normal, see Fig. 6). The present polar scan analysis revealed the epitaxial growth of the B-type $NiSi_2$ islands by post-annealing at 600 and 700 °C. The variation of $NiSi_2$ orientation as a function of deposited Ni thickness was investigated in detail by Tung [9] by means of low energy electron diffraction and transmission electron microscopy. According to his report, thin $NiSi_2$ layers formed with 1–5 Å Ni are predominantly type B oriented.

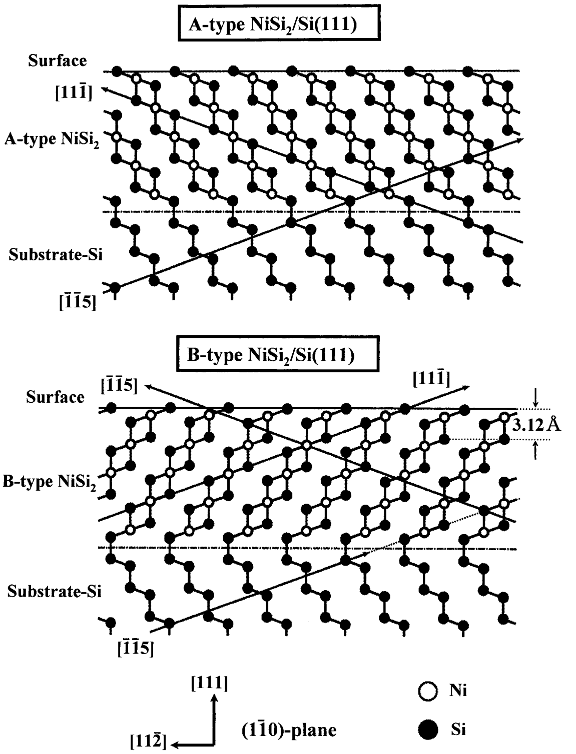

Fig. 6. Cross sections of A-type $NiSi_2$(1 1 1)/Si(1 1 1) (upper) and B-type-$NiSi_2$(1 1 1)/Si(1 1 1) (lower) viewed from $[1\,\bar{1}\,0]$-axis.

4. Summary

Structure change of Ni(1 ML)/Si(1 1 1) by post-annealing was observed by RHEED, AFM, MEIS

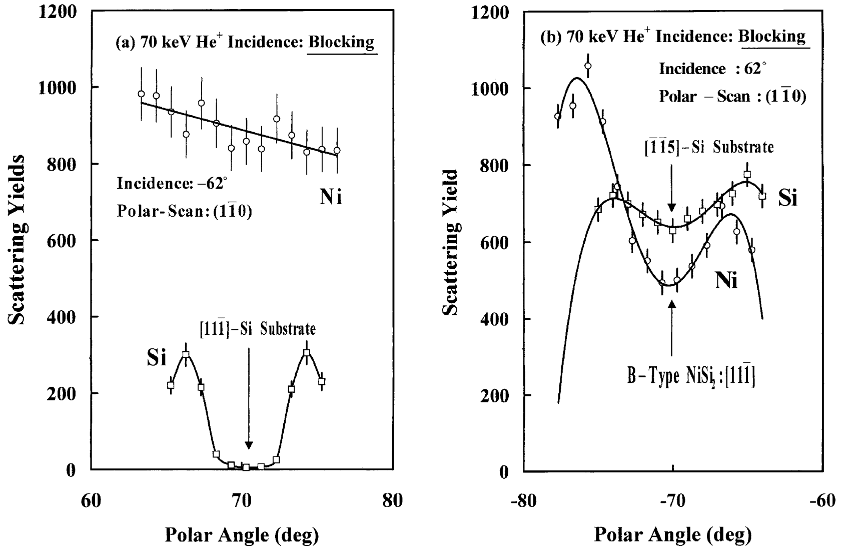

Fig. 7. 70 keV He$^+$ incidence at 62° from surface normal (random) for 600 °C-annealed sample. (a) Polar scan around $[11\bar{1}]$-axis in $(1\bar{1}0)$ plane of Si substrate for scattering component from the second-layer Ni atoms (including a small contribution from the fifth-layer Ni) and for scattering component from the Si substrate. (b) Polar scan around $[\bar{1}\bar{1}5]$-axis in $(1\bar{1}0)$ plane of Si substrate for scattering component from the second-layer Ni (including a small contribution from the fifth-layer Ni) and for scattering component from the Si substrate.

and PES using SR-light. All the analyses were performed in situ under UHV condition ($\leqslant 2 \times 10^{-10}$ Torr) except for the AFM observation. All the results obtained by RHEED, AFM, PES and MEIS are listed up in Table 1. The AFM observation revealed dramatic change of the surface morphology after the Ni deposition at RT followed by annealing at 400, 600, 700 and 800 °C in UHV. MEIS using 70 keV He$^+$ ions analyzed the depth profiles of Ni and the crystallographic structure of the Ni-composites formed by post-annealing. The valence band and the Si-2p and Ni-3p core level analyses were performed with SR-photon energy of 40, 114 and 130 eV and identified the phases formed by Ni(1 ML)-deposition at RT and by post-annealing. The surface morphology change studied by the present experiment is summarized as follows. The Ni atoms deposited at RT coalesced to make ridge-like stripes perpendicular to steps and formed fine clusters in some places. The average height of the ridges is about 1.5 Å. The UPS analysis suggests that the fine clusters and/or ridges take the NiSi phase. By 400 °C-annealing, Ni atoms coalesced to form Ni–silicide islands on upper terrace sides at step edges. The height of relatively large islands is 6.5 Å, corresponding to 2-triple layers of $NiSi_2$. At this stage, both NiSi (small) and $NiSi_2$ (large) islands were formed and the amount of the residual Ni atoms was 0.81 ML. From the shape and location, the larger islands seem to be a precursor state of the $NiSi_2$ islands observed for the 600 °C-annealed sample. Annealing at 600 and 700 °C led to growth of the B-type $NiSi_2$ islands with average height of 4- and 6-triple layers, respectively. Nearly half the deposited Ni atoms (0.5 ML) was lost from the surface region by post-annealing at 600 °C for 2 min. After annealing at 800 °C, three-fourth of the deposited Ni atoms were dissipated from the surface and the dominant surface structure was the 1 × 1-RC accompanied by a small amount of the $\sqrt{19} \times \sqrt{19}$ phase. A small excess (about 0.1 ML) of the Ni atoms which were segregated to the surface probably formed fine clusters of $NiSi_2$.

Acknowledgements

The authors would like to thank Prof. T. Nakada for useful discussion and comments on the

AFM observation. Special thanks are also due to T. Okazawa, S. Semba, O. Kitamura and Y. Yagi for their help in carrying out the MEIS measurements.

References

[1] L.J. Chen, K.N. Tu, Mater. Sci. Rep. 6 (1991) 53.
[2] H. von Känel, Mater. Sci. Rep. 8 (1991) 193.
[3] S. Mantl, Nucl. Instrum. Meth. B 84 (1994) 127.
[4] R.T. Tung, in: T.S. Moss (Ed.), Handbook on Semiconductors, vol. 3B, North-Holland, Amsterdam, 1994 (Chapter 25).
[5] K. Maex, M. van Rossum, Properties of Metal Silicides, Short Run Press, London, 1995.
[6] R.T. Tung, J.C. Bean, J.M. Gibson, J.M. Poate, D.C. Jacobson, Appl. Phys. Lett. 40 (1982) 684.
[7] R.T. Tung, J.M. Gibson, J.M. Poate, Phys. Rev. Lett. 50 (1983) 429.
[8] R.T. Tung, Phys. Rev. Lett. 52 (1984) 461.
[9] R.T. Tung, J. Vac. Sci. Technol. A 5 (1987) 1840.
[10] F. Comin, J.E. Rowe, P.H. Citrin, Phys. Rev. Lett. 51 (1983) 2401.
[11] E.J. van Loenen, J.F. van der Veen, F.K. LeGoues, Surf. Sci. 157 (1985) 1.
[12] T.L. Porter, C.S. Chang, U. Knipping, I.S.T. Tsong, Phys. Rev. B 36 (1987) 9150.
[13] P.A. Bennett, A.P. Johnson, B.N. Halawith, Phys. Rev. B 37 (1988) 4268.
[14] T. Ichinokawa, T. Tani, A. Sayama, Surf. Sci. 219 (1989) 395.
[15] J. Vrijmoeth, P.M. Zagwijn, J.W.M. Frenken, J.F. van der Veen, Phys. Rev. Lett. 67 (1991) 1134.
[16] P.A. Bennett, M. Copel, D. Cahill, J. Falta, R.M. Tromp, Phys. Rev. Lett. 69 (1992) 1224.
[17] S.A. Parkin, M.Y. Lee, P.A. Bennett, J. Vac. Sci. Technol. A 13 (1995) 1589.
[18] S.A. Parkin, M.Y. Lee, P.A. Bennett, Surf. Sci. 356 (1996) 53.
[19] M. Yoshimura, S. Shinabe, T. Yao, Surf. Sci. 357–358 (1996) 917.
[20] L. Gregoratti, S. Günther, J. Kovaĉ, L. Casalis, M. Marsi, M. Kiskinova, Phys. Rev. B 57 (1998) R6799.
[21] L. Gregoratti, S. Günther, J. Kovaĉ, M. Marsi, R.J. Phaneuf, M. Kiskinova, Phys. Rev. B 59 (1999) 2018.
[22] Y. Kido, H. Namba, T. Nishimura, A. Ikeda, Y. Yan, A. Yagishita, Nucl. Instrum. Meth. B 136–138 (1998) 798.
[23] H. Namba, M. Obara, D. Kawakami, T. Nishimura, Y. Yan, A. Yagishita, Y. Kido, J. Synchrotron Rad. 5 (1998) 557.
[24] Y.J. Chabal, D.R. Hamann, J.E. Rowe, M. Schlüter, Phys. Rev. B 25 (1982) 7598.
[25] A. Franciosi, J.H. Weaver, F.A. Schmidt, Phys. Rev. B 26 (1982) 546.
[26] O. Bisi, C. Calandra, U. del Pennino, P. Sassaroli, S. Valeri, Phys. Rev. B 30 (1984) 5696.
[27] C.J. Karlsson, E. Landemark, Y.-C. Chao, R.I.G. Uhrberg, Phys. Rev. B 50 (1994) 5767.
[28] T. Nishimura, Y. Hoshino, H. Namba, Y. Kido, Nucl. Instrum. Meth. A 467–468 (2001) 1237.
[29] For exampleS. Hüfner (Ed.), Photoelectron Spectroscopy, Springer, Berlin, 1994 (Chapter 4).
[30] T. Nishimura, A. Ikeda, Y. Kido, Rev. Sci. Instrum. 69 (1998) 1671.
[31] Y. Kido, T. Nishimura, Y. Hoshino, H. Namba, Nucl. Instrum. Meth. B 161–163 (2000) 371.